Chemical characterization of nanoparticles and volatiles present in mainstream hookah smoke

Véronique Perraud, Michael J. Lawler, Kurtis T. Malecha, Rebecca M. Johnson, David A. Herman, Norbert Staimer, Michael T. Kleinman, Sergey A. Nizkorodov & James N. Smith

Taylor & Francis
Taylor & Francis Group

Chemical characterization of nanoparticles and volatiles present in mainstream hookah smoke

Véronique Perraud[a] (iD), Michael J. Lawler[a] (iD), Kurtis T. Malecha[a] (iD), Rebecca M. Johnson[b] (iD), David A. Herman[b] (iD), Norbert Staimer[c], Michael T. Kleinman[b] (iD), Sergey A. Nizkorodov[a] (iD), and James N. Smith[a] (iD)

[a]Department of Chemistry, University of California, Irvine, California, USA; [b]School of Medicine, University of California, Irvine, California, USA; [c]Department of Epidemiology, University of California, Irvine, California, USA

ABSTRACT

Waterpipe smoking is becoming more popular worldwide and there is a pressing need to better characterize the exposure of smokers to chemical compounds present in the mainstream smoke. We report real-time measurements of mainstream smoke for carbon monoxide, volatile organic compounds and nanoparticle size distribution and chemical composition using a custom dilution flow tube. A conventional tobacco mixture, a dark leaf unwashed tobacco, and a nicotine-free herbal tobacco were studied. Results show that carbon monoxide is present in the mainstream smoke and originates primarily from the charcoal used to heat the tobacco. Online measurements of volatile organic compounds in mainstream smoke showed an overwhelming contribution from glycerol and its decomposition products. Gas phase analysis also showed that very little filtration of the gas phase products is provided by the percolation of mainstream smoke through water. Waterpipe smoking generated high concentrations of 4–100 nm nanoparticles, which were mainly composed of sugar derivatives and especially abundant in the first 10 min of the smoking session. These measured emissions of volatiles and particles are compared with those from a reference cigarette (3R4F) and represent the equivalent of the emission of one or more entire cigarettes for a single puff of hookah smoke. Considerations related to the health impacts of waterpipe smoking are discussed.

1. Introduction

Waterpipe smoking (also known as *narghile* or *hookah* depending on cultural traditions) is a way of smoking tobacco in which air is passed over heated charcoal, which transfers its thermal energy to the tobacco located in the head of the hookah underneath the charcoal, producing smoke. The smoke, composed of both charcoal burning products and compounds released from the heated tobacco, is entrained down the stem of the waterpipe and bubbles through water by the action of puffing on the waterpipe hose before being inhaled by the smoker. The attraction for this mode of smoking tobacco is driven by the variety of available tobacco flavors, the absence of visible side-stream smoke, the social aspect of smoking in group, the misconception that waterpipe smoking is less harmful than smoking cigarettes due to the possible filtration effects provided by the water, and the prevalence of

advertised nicotine-free tobacco (Akl et al. 2013; Aljarrah, Ababneh, and Al-Delaimy 2009; Salloum et al. 2015).

The number of waterpipe smokers is significant and on the rise in the United States (Cobb et al. 2010; Sutfin et al. 2014) and worldwide (Martinasek, McDermott, and Martini 2011; Maziak 2011). Waterpipe use is growing most dramatically among university students and other young adults (Aslam et al. 2014; Grekin and Ayna 2008; Primack et al. 2008). Smith et al. (2011) reported that the usage of waterpipe by all adults (ages > 18) had increased by 41.8% (men) and 47.4% (women) from 2005 to 2008 in California, and by young adults (ages 18–24) by about 24%. In a different study, Grekin and Ayna (2012) showed that 1 out of 5 college students in the United States and Europe had smoked waterpipes in 2011, and 1 out of 4 college students in the Middle East had smoked waterpipes in the last month prior

the survey. Furthermore, data from a recent National Youth Tobacco Survey (NYTS) (Jamal et al. 2017) reported an increase in the usage of waterpipe among high school (4.1% to 4.8%) and middle school students (1.0% to 2.0%) in the United States from 2011 to 2016. As a consequence, there is a growing concern for understanding impacts of waterpipe smoking on human health and needs for regulations (Maziak 2011; World Health Organization 2015).

Numerous carcinogens and toxic pollutants have been previously identified in mainstream hookah smoke (smoke directly inhaled by the smoker) including nicotine (Katurji et al. 2010; Schubert et al. 2011a; Shihadeh 2003; Shihadeh and Saleh 2005; Shihadeh et al. 2012), nitrosamines (Schubert et al. 2011a), aromatic amines (Schubert et al. 2011b), polycyclic aromatic hydrocarbons (PAHs) (Hammal et al. 2015; Monzer et al. 2008; Schubert et al. 2011a; Sepetdjian, Shihadeh, and Saliba 2008; Shihadeh and Saleh 2005; Shihadeh et al. 2012), volatile carbonyl compounds (Al Rashidi, Shihadeh, and Saliba 2008; Hammal et al. 2015; Schubert et al. 2012b; Shihadeh et al. 2012), benzene (Schubert et al. 2015), phenols (Schubert et al. 2015; Sepetdjian et al. 2013), furans (Schubert et al. 2012a), carbon monoxide (CO) (Hammal et al. 2015; Katurji et al. 2010; Monn et al. 2007; Monzer et al. 2008; Schubert et al. 2011a; Shihadeh et al. 2014; Shihadeh and Saleh 2005; Shihadeh et al. 2012), nitric oxide (Hammal et al. 2015; Shihadeh et al. 2014; Shihadeh et al. 2012), and heavy metals (Schubert et al. 2015; Shihadeh 2003). In addition, waterpipe tobacco smoking has been associated with negative impacts on the respiratory and cardiovascular systems, periodontal diseases, low birth weight, cancers, and a higher risk for infection due to sharing the mouthpiece (Akl et al. 2010; Aslam et al. 2014; El-Zaatari, Chami, and Zaatari 2015; Fakhreddine, Kanj, and Kanj 2014; Kim, Kabir, and Jahan 2016; Rezk-Hanna and Benowitz 2018).

Carbon monoxide is well-known for binding to the hemoglobin to form carboxyhemoglobin (CO-Hb) and thus inhibiting the hemoglobin's ability to bind with vital oxygen. Several acute CO poisoning cases have been previously reported for waterpipe smokers where levels of CO-Hb were almost always higher than 20% of total hemoglobin (Cavus et al. 2010; Eichorn et al. 2018; La Fauci et al. 2012; Lim, Lim, and Seow 2009; Retzky 2017; Veen 2016). CO levels are influenced by the choice of heat source, and the design of the waterpipe. For example, Monzer et al. (2008) reported that CO levels in mainstream hookah smoke can be reduced by a factor of 10 when using a custom-built electrical heater instead of charcoal, and Saleh and Shihadeh (2008)

reported that switching from plastic to more permeable leather hose would reduce the CO concentration ultimately inhaled by the smoker by about half; however, the CO emitted directly from the charcoal and that escaping from the mainstream smoke will still be present in the air surrounding the smoker (sidestream smoke).

All previously reported chemical investigations relied on off-line analysis techniques, which are often time-consuming, lack sensitivity towards low-volatility gases and small particles, and have primarily focused on total toxic pollutant and particle yields. Additionally, off-line analyses often integrate over an entire smoking session, so examinations of the time evolution of the concentration or composition in the mainstream smoke during session were not possible. The present work introduces a new approach to the study of waterpipe mainstream smoke by allowing online measurements of CO, volatile organic compounds (VOCs) and particle size distributions and chemical composition. Thermal Desorption Chemical Ionization Mass Spectrometry, TDCIMS (Smith et al. 2004), is applied for the first time for characterizing waterpipe mainstream smoke chemical composition, and this is the first report of real-time size distributions of particles in mainstream waterpipe smoke. Although online measurements of VOCs using proton-transfer-reaction mass spectrometry (PTR-MS) has been previously applied to smoke from cigarettes (Brinkman et al. 2015; Gordon et al. 2011) and e-cigarettes (Blair et al. 2015; Breiev et al. 2016), this is the first application of this technique to mainstream waterpipe smoke.

Our study compared the emissions from a glass waterpipe using three different tobacco mixtures, including one unwashed dark leaf tobacco and a nicotine-free herbal tobacco, following a modified Beirut protocol smoking pattern (4 s puff duration, 2 min^{-1} puff frequency, 860 ml puff volume). These conditions were well within the range of conditions recorded from a cohort of waterpipe smokers in Beirut, Lebanon (Shihadeh 2003; Shihadeh et al. 2004) from which the Beirut protocol was established, and very similar to recent studies performed in the US involving established waterpipe users (Brinkman et al. 2018; Kim et al. 2016). Typical waterpipe smoking duration recorded in natural and laboratory settings range between ∼20 min up to > 60 min (Jawad et al. 2019; Maziak et al. 2009; Shihadeh 2003). In addition, acute health effects studies are oftentimes reported for a 30 min smoking duration (El-Zaatari, Chami, and Zaatari 2015). As a result, a representative 30 min smoking session duration was selected for this study. All reported concentrations are given hereafter as the concentrations of each toxic pollutant directly emitted

from the waterpipe during smoking, i.e., after accounting for the dilution necessitated by the measurement devices. The emissions from waterpipe experiments were directly compared with emissions from a reference cigarette (3R4F), also measured in this work, and potential risks and impacts on health are discussed.

2. Material and methods

A brief description of the experimental procedure is provided below, but further details can be found in the online supplementary information (SI), including the complete waterpipe smoking protocol and the details of the instrument operations. All smoking sessions were performed using the same waterpipe (Anahi Smoke, model "Fantasy") which was constructed entirely of glass for ease in cleaning (SI Figure S1). At the beginning of each experiment, 10 g of tobacco were packed loosely in the head of the waterpipe, which is wrapped with a pre-punched aluminum foil (Starbuzz Tobacco Inc., Starbuzz Premium foil). Three different tobacco mixtures were tested in this study, including a conventional tobacco (Al Fakher, apple flavor), a nicotine-free herbal tobacco (Hydro Herbal, banana flavor) and an unwashed dark leaf tobacco (Vintage by Starbuzz, Dark Mist, blackberry flavor). Then, three charcoal cubes (100% natural coconut husks; Black Diamond) were lighted and placed atop the head to uniformly heat the tobacco (SI Figure S1). The smoking session lasted for 30 min, using the following smoking regimen: puff frequency, 2 puff/min; puff duration, 4 s; puff volume, 860 mL. Control experiments including no charcoal (or charcoal only), no water (or water only), or no tobacco, were also performed to identify the sources of both the organic gases and particles. Lastly, as glycerol is a major component of the tobacco formulations, a control experiment with pure glycerol (EMD Millipore, ACS grade) instead of the tobacco was conducted.

A fast flow dilution system was developed to dilute the mainstream smoke emission of the waterpipe to levels manageable by our analytical instruments as well as to provide continuous flow conditions that are needed for stable instrument operation. A diagram of the system is presented in Figure 1. Additional details on the dilution system can be found in SI, including the characterization of the transmission efficiency of the particles through the dilution system (SI Figures S2–S4). The total dilution factor of the waterpipe emission sampled through the entire system ranged

from 241 to 325. An average value of 276 ± 34 (1σ) is used hereafter for all calculations.

The mainstream smoke sampling train was composed of a series of dedicated instruments including a scanning mobility particle sizer (SMPS; TSI) to measure size distribution of particles, a CO monitor (Thermo Fisher Scientific, model 48i) and two mass spectrometers measuring the volatiles (PTR-ToF-MS, model 8000, Ionicon Analytik) (Jordan et al. 2009) and the particle chemical composition (TDCIMS) (Lawler et al. 2018; Smith et al. 2004). All details of the instrumentation operation are given in SI. Additionally, two relative humidity and temperature probes (Vaisala Corp., model HMP110) were placed at the entrance and exit of the dilution system.

Although this study focused on the mainstream emissions from waterpipe, a comparative study with one type of reference cigarette (3R4F, University of Kentucky) was conducted using the same fast flow dilution system. This type of cigarette has a filter ventilation of 20%, high tar (9.40 mg/cig.) and a nicotine content of 0.73 mg/cig (Sampson et al. 2014). Details of the smoking regimen and protocol are provided in SI.

3. Results and discussion

For all the waterpipe experiments, an optically dense white aerosol formed within the waterpipe at the first puff, and was maintained throughout the 30-min smoking session. No side stream smoke was observed in any experiments. The tobacco mixtures were all weighed at the end of the sessions, and an average loss of 2.2 ± 0.4 g (out of the initial 10 g) was measured. Control experiments performed in absence of water showed a similar behavior. Experiments carried out with ~4 g of pure liquid glycerol instead of the tobacco only yielded a loss of ~0.2 g of glycerol over the 30-min smoking session.

In a separate experiment, the temperature in the head of the hookah (i.e., the place where the tobacco resides) was measured using a thermocouple (Omega, probe type K). The temperature ranged from 265°C to 318°C during the 30-min smoking session. Although three charcoal cubes were necessary to uniformly heat the tobacco mixture, the temperature recorded in this study was in agreement with a previous measurement using one easy-lighting briquette (Monzer et al. 2008). Measurements indicated that at every puff, the temperature inside the head of the hookah decreased by ~50°C for the duration of the puff (as sample air was drawn into the head of the hookah) and then rose up
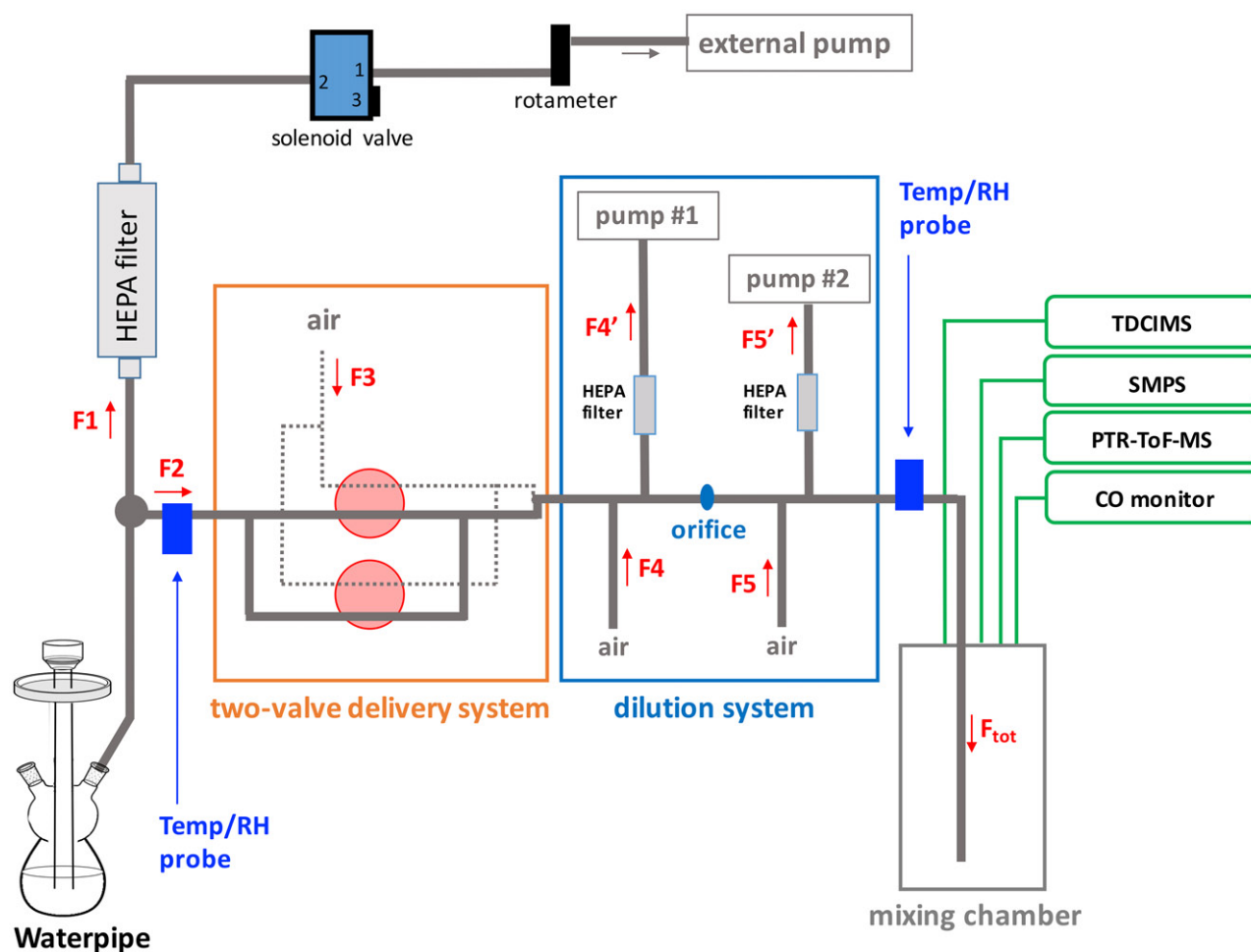
Figure 1. Diagram of the fast flow dilution system used in the waterpipe smoking experiments. A fraction of the total puff flow is sampled through the dilution system (F2, ~3 L min^{-1}) while the rest is pumped off (F1, ~10 L min^{-1}). Dilution air from a purge air generator is provided in the two stages of dilution and the flows in and out are balanced (F4 = F4′ and F5 = F5′). Flows F2 and F3 are equal and governed by the sum of the analytical instruments connected at the end of the mixing section as F2 = F3 = F_{total} = F_{TDCIMS} + F_{SMPS} + $F_{PTR-ToF-MS}$ + F_{CO}.

between puffs. For comparison, the temperature (and RH) of the mainstream smoking exiting the waterpipe and at the outlet of the dilution system is presented in SI Figure S5.

3.1. Gas phase measurements

3.1.1. Carbon monoxide

Due to instrument malfunction, the CO monitor was available for only selected experiments with the conventional tobacco and for the 3R4F reference cigarettes. No significant differences were observed for the full waterpipe experiment (tobacco + water + charcoal) and the controls (no water; charcoal only). A separate experiment was carried out without charcoal (no heat) showing no detectable CO, confirming that CO mainly came from the combustion of the charcoal, consistent with previous reports (Monzer et al. 2008). After correcting for calibration bias and dilution, an average mixing ratio of 2.1 ($\pm$0.6) $\times$ 10^3 ppm of CO was observed from the waterpipe mainstream smoke, compared to 3.3 ($\pm$0.3) $\times$ 10^4 ppm from the cigarette smoke. The estimated mass of CO inhaled in 1 puff of mainstream smoke was 2.0 ($\pm$0.6) mg and 1.4 ($\pm$0.1) mg respectively for the hookah and cigarette smoke. Those results are in agreement with previously reported CO dose from mainstream smoke by Monn et al. (2007). If this dose is integrated over the entire waterpipe smoking session (i.e., 60 puffs), a total amount of 121 mg of CO is expected to be inhaled per session. For comparison with literature values summarized in Shihadeh et al. (2015), our measurement was multiplied by a factor of 2 to account for the difference in smoking time (all reported studies were for ~1hr smoking session), and yield a total of 242 mg CO emitted, which is well within the range reported by previous studies (e.g., 57–367 mg/session). Likewise, the integrated dose of CO from one cigarette
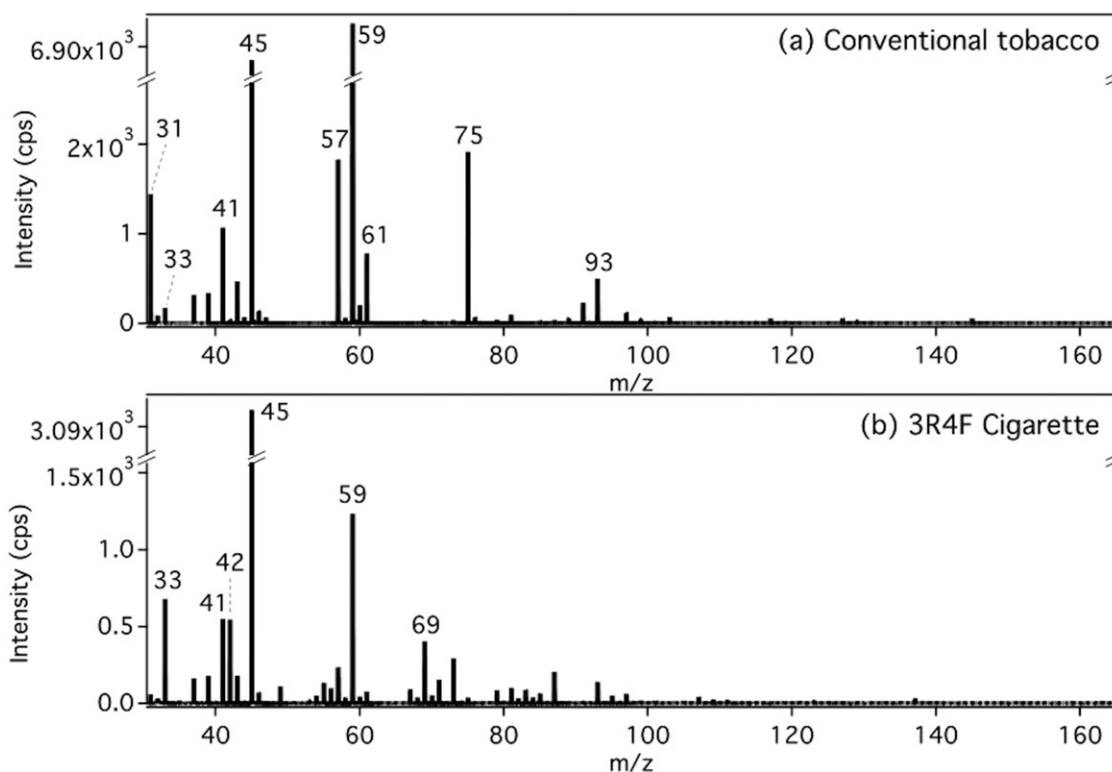
Figure 2. Typical unit mass resolution PTR-ToF-MS mass spectra from (a) the waterpipe mainstream smoke of the conventional tobacco and (b) the 3R4F reference cigarette. All spectra were collected at the end of the smoking session (the last 10 puffs for the waterpipe sample, and the last puff for the cigarette sample) and the background signal has been subtracted out.

was 9.7 mg, which is also in agreement with previously reported values (Eldridge et al. 2015; Roemer et al. 2012). Therefore, the dose of CO from a single waterpipe smoking session was equivalent to a dose of CO from 12 references cigarettes.

3.1.2. Volatile organic compound measurements

Figures 2a–b represents typical background subtracted mass spectra obtained from the conventional tobacco mixture and the 3R4F reference cigarette, respectively (the background corresponds to the baseline signal intensity before the smoking session started). For comparison, the mass spectra for the other tobacco mixtures are presented in SI Figure S6.

All spectra derived from hookah mainstream smoke show the distribution of VOC-derived ions observed during the last 5 min (10 puffs) of the smoking session. Ions at nominal m/z 41, 43, 45, 57, 59, 61, 75, and 93 were the major common ions observed for all three tobacco mixtures (Figure 2a and SI Figure S6). Table 1 reports the likely attributions for the ions observed in this study. These attributions are consistent with previously reported assignments from PTR-MS measurements (de Gouw and Warneke 2007; Yuan et al. 2017), and in addition, each m/z observed

in our experimental mass spectra matched the exact mass of the assigned chemical to within 3 mDa, which is an acceptable error on accurate mass determination for m/z up to 1000 Da (Greaves and Roboz 2014).

SI Figure S7 illustrates the advantage of using a high resolution time-of-flight mass spectrometer that allows the differentiation between molecular formulas having the same nominal mass. With the exception of m/z 91 (glyceraldehyde), 93 (glycerol) and 163 (nicotine), all compounds have been previously reported in biomass burning samples (Brilli et al. 2014; Bruns et al. 2017; Fitzpatrick et al. 2007; Karl et al. 2007; Muller et al. 2016; Stockwell et al. 2015; Warneke et al. 2011), so it is not surprising to observe them in this study.

It is interesting to note that all three tobaccos show similar patterns in the relative intensity of the detected ions (SI Table S1), with the exception of the conventional tobacco which exhibits a larger contribution from m/z 59.049, 41.039, and 31.018 than the other two tobaccos. The differences between tobaccos are likely due to the differences in flavoring. The nicotine-free herbal tobacco shows, in general, a higher ion intensity at every major ion, including m/z 117.055 ($[C_5H_8O_3 + H]^+$) that is clearly visible in the

Table 1. Ions observed in the PTR-ToF-MS mass spectra from the waterpipe mainstream smoke samples (conventional tobacco; nicotine-free herbal tobacco; dark leaf unwashed tobacco) and the 3R4F reference cigarette.

Nominal m/z	Exact m/z	Empirical formula	Assigned compound
31	31.018	$[CH_2O + H]^+$	Formaldehyde
33	33.033	$[CH_4O + H]^+$	Methanol
41	41.039	$[C_3H_4 + H]^+$	Propadiene[a]
42	42.034	$[C_2H_3N + H]^+$	Acetonitrile[b]
43	43.018	$[C_2H_2O + H]^+$	Acetic acid fragment,[c] glycolaldehyde fragment,[c] hexyl acetate fragment[d]
	43.054	$[C_3H_6 + H]^+$	Propylene[a]
45	45.033	$[C_2H_4O + H]^+$	Acetaldehyde
47	47.013	$[CH_2O_2 + H]^+$	Formic acid
	47.049	$[C_2H_6O + H]^+$	Ethanol
57	57.033	$[C_3H_4O + H]^+$	Acrolein, hexyl acetate fragment[d]
	57.070	$[C_4H_8 + H]^+$	Butene[a,b]
59	59.049	$[C_3H_6O + H]^+$	Acetone, propionaldehyde, methyl vinyl ether
61	61.028	$[C_2H_4O_2 + H]^+$	Acetic acid, hydroxyacetaldehyde (glycolaldehyde)
69	69.033	$[C_4H_4O + H]+$	Furan
	69.070	$[C_5H_8 + H]^+$	Isoprene[a]
75	75.044	$[C_3H_6O_2 + H]^+$	Hydroxyacetone (acetol), 3-hydroxypropanal, 1,3-dihydroxypropene, glycerol fragment (-H2O)
79	79.054	$[C_6H_6 + H]^+$	Benzene[e]
91	90.948	$FeOH(H_2O)^+$	Intrinsic ion from the PTR-ToF-MS ion source[f]
	91.039	$[C_3H_6O_3 + H]^+$	Glyceraldehyde, lactic acid
	91.054	$[C_7H_6 + H]^+$	Fragment from benzyl compounds[g]
93	93.055	$[C_3H_8O_3 + H]+$	Glycerol
	93.070	$[C_7H_8 + H]^+$	toluene
117	117.055	$[C_5H_8O_3 + H]^+$	1-acetoxyacetone[h]
163	163.123	$[C_{10}H_{14}N_2 + H]^+$	Nicotine

[a]Correspond to compounds often found in biomass burning samples (refer to Brilli et al. (2014) and references therein); significant in the cigarette samples.
[b]Not present in the waterpipe mainstream smoke.
[c]Refer to Baasandorj et al. (2015) and Haase et al. (2012).
[d]Hexyl acetate was found in biomass burning (Brilli et al. 2014) as well as in numerous waterpipe tobacco mixtures acting as a flavoring agent (Schubert et al. 2013).
[e]Significant in the cigarette samples; ethylbenzene fragment can also contribute to m/z 79 (Rogers et al. 2006), however, ethylbenzene (m/z 107) was only observed in the cigarette sample (see SI Figure S7).
[f]Refer to Schroder et al. (2008).
[g]No clear source for the tropylium ion ($C_7H_7^+$) could be found here, although Sovova et al. (2011), reported that phytogenic compounds such as benzyl acetate or benzyl benzoate can produce efficiently this ion upon SIFT-MS ionization. Benzyl acetate was found in numerous flavor waterpipe tobacco mixtures (Schubert et al. 2013).
[h]Previously identified in pine wood combustion samples (Fitzpatrick et al. 2007) and African grass (Stockwell et al. 2015).

spectra. We assigned this ion to 1-acetoxyacetone (Table 1) because it was previously found in pine wood combustion samples (Fitzpatrick et al. 2007).

Mass spectra from control experiments, which include experiments performed without any tobacco (charcoal + water only), with the conventional tobacco but no charcoal (no heat) and only glycerol (replacing the tobacco) are given in SI Figure S8. The major common ions (nominal m/z 43, 45, 57, 61, and 75) observed in the waterpipe mainstream smoke were common to all spectra, including that of glycerol (propane-1,2,3-triol). Upon thermal decomposition, glycerol has been reported to form not only two major products, namely acetaldehyde (C_2H_4O, MW = 44 g mol^{-1}) and acrolein (C_3H_4O, MW = 56 g mol^{-1}), but also 3-hydroxypropanal ($C_3H_6O_2$, MW = 74 g mol^{-1}), 1-hydroxypropan-2-one ($C_3H_6O_2$, MW = 74 g mol^{-1}), hydroxyacetone (or acetol; $C_3H_6O_2$, MW = 74 g mol^{-1}), glycolaldehyde ($C_2H_4O_2$, MW = 60 g mol^{-1}), and acetic acid ($C_2H_4O_2$, MW = 60 g mol^{-1}) (Corma et al. 2008; Hemings et al. 2012; Jensen, Strongin, and

Peyton 2017; Katryniok et al. 2010; Martinuzzi et al. 2014; Nimlos et al. 2006). Ionization of these compounds in the PTR-ToF-MS ion source would give the observed $[M + H]^+$ ions. Both acetic acid and glycolaldehyde are known to fragment under typical PTR-MS conditions such as the ones applied here, to give an additional fragment at m/z 43.018 ($C_2H_3O^+$) (Baasandorj et al. 2015). Though, acetic acid is thought to be formed from secondary oxidation process (Jensen, Strongin, and Peyton 2017; Katryniok et al. 2010), it is more likely that the peaks at m/z 61/43 are due to glycolaldehyde instead. Further evidence for this assignment is the presence of a minor peak at m/z 91.039 attributed to glyceraldehyde (SI Figure S7), which was previously proposed as an intermediate in the decomposition process of glycerol leading to glycolaldehyde. (Jensen, Strongin, and Peyton 2017).

In addition, experiments and theoretical calculations demonstrated that the protonated $[M + H]^+$ ion of glycerol at nominal m/z 93 can itself undergo dehydration to yield ions at m/z 75, 61, 57, 45, and 43

(Dass 1994; Nimlos et al. 2006). Note, although the glycerol parent ion at m/z 93.055 was observed in the waterpipe mainstream smoke of all three tobacco, it was not detectable in the glycerol experiment due to a very low concentration of glycerol in the gas phase sampled (but was observed for pure glycerol particles measured in separate experiments; SI Figure S8d). Alcohols are known to readily fragment by losing a molecule of water upon proton transfer reaction ionization process via reaction with H_3O^+ (Spanel and Smith 1997) and only at high concentration the parent peak was observable. In brief, glycerol related peaks overwhelm the mass spectra of the gas phase products emitted by the waterpipe during smoking, and this is not surprising as it is used as a wetting agent or humectant for the tobacco (Rainey et al. 2013; Schubert et al. 2011a, 2012a, 2012b). Our results are also consistent with a previous study by Schubert et al. (2011a) in which significant amount of glycerol in waterpipe mainstream smoke was measured (up to 423 mg/session).

As seen in Figure 2b, the PTR-MS spectrum of mainstream smoke from the waterpipe experiment is very different from that of the 3R4F reference cigarette smoke. The latter shows a different distribution of ions, including significant signal intensities at m/z 42.034 (acetonitrile), 33.034 (methanol), 69.070 (isoprene) and 79.054 (benzene). While methanol is visible in the conventional tobacco mass spectra, acetonitrile is not present in any of the waterpipe samples as illustrated by the high resolution mass spectra of nominal m/z 42 (SI Figure S7). A peak at m/z 69.034 ($[C_4H_4O+H]^+$) is also observed as a minor peak in the MS spectra for the waterpipe mainstream smoke, attributed to a furan compound, while in the cigarette smoke, it is attributed to isoprene (m/z 69.0704, $[C_5H_8+H]^+$) (Table 1, SI Figure S7). Present in cigarette smoke, a peak at m/z 79.054 attributed to benzene was also identified as a minor contributor of hookah mainstream smoke (SI Figure S9) consistent with previous studies (Schubert et al. 2015; Shihadeh et al. 2015). Although a small fraction of benzene found in the hookah smoke was emitted from the charcoal only, most of the benzene measured in the conventional and nicotine-free herbal tobacco originated from the tobacco itself upon heating (SI Figure S9). Lastly, an ion at m/z 163.123 indicative of nicotine ($C_{10}H_{14}N_2$) was observed in the cigarette mainstream smoke sample. Nicotine was also detected in the waterpipe mainstream smoke of both the conventional and dark leaf unwashed tobacco as a minor product, and none was measured for the nicotine-free

herbal tobacco (SI Figure S7). Instead, a peak at m/z 163.097 was observed for the herbal tobacco, and assigned to $[C_7H_{14}O_4+H]^+$ ion.

SI Figure S10 represents the evolution of the PTR-ToF-MS mass spectra as a function of smoking time (each mass spectrum corresponding to an average over 10 puffs) for the conventional tobacco runs performed under 'normal' conditions (charcoal + tobacco + water) and for control experiments without water present in the waterpipe. The time evolution showed that, in both cases, the signal intensity of each ion increased as a function of smoking time (number of puffs) to reach a plateau, and no significant differences exists with and without water present in terms of ion distribution or intensities. However, care should be taken to interpret the increase of the signal as a function of time as a true emission profile from the waterpipe, as instrument delays have been observed previously to happen with sampling tubes (Mikoviny, Kaser, and Wisthaler 2010; Pagonis et al. 2017).

Two exceptions exist when comparing experiments ran *with* and *without* water in the waterpipe bowl, which are the ions observed at m/z 33.034 and 47.049 (attributed to methanol and ethanol respectively). Those ions appear to be particularly sensitive to the presence of water, for which a strong filtration effect is observed as illustrated in the expanded mass spectra in SI Figure S11. This observation is consistent with their respective Henry's law constant (K_H), which are 2.03 and 1.7 mol m^{-3} Pa^{-1} respectively (Sander 2015). It is not surprising to observe no filtration effect for carbonyls compounds measured in this study as their K_H values by comparison is much smaller with average values of, for example, 0.14 mol m^{-3} Pa^{-1} for acetaldehyde and 0.10 mol m^{-2} Pa^{-1} for acrolein (Sander 2015). Following a similar analysis, Al Rashidi, Shihadeh, and Saliba (2008) previously demonstrated that acetaldehyde, acrolein, propionaldehyde and methacrolein all remained in the gas phase, while formaldehyde, the most soluble of the carbonyl compounds measured, was found in the particle phase due to its much higher solubility, $K_H \sim 43$ mol m^{-3} Pa^{-1} (Sander 2015).

Although extremely soluble with $K_H \sim 7.2$ x 10^3 mol m^{-3} Pa^{-1} (Sander 2015), the small nicotine signal observed at m/z 163.125 was not noticeably affected by the presence of water (SI Figure S11) suggesting a very small trapping effect. Overall, our observations show that water does not act as a filter for volatile organic compounds under our smoking conditions.
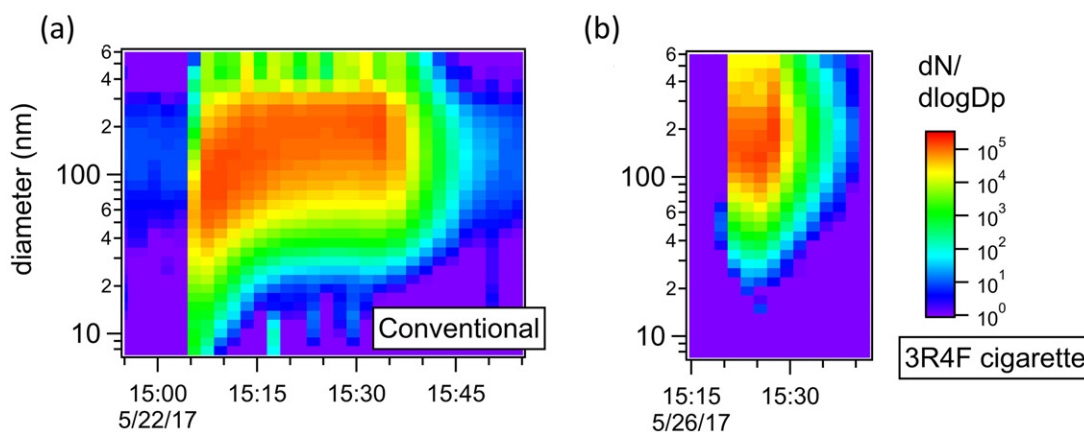
persistent mode around 10 nm was observed throughout the experiments, distinct from the other tobaccos. This mode indicates that there was nucleation of new particles from the mainstream smoke throughout the smoking session. This observation is consistent with the TDCIMS measurements described in detail below in that organic compounds from the dark leaf unwashed tobacco desorbed from the Pt wire at a later time compared to the other two tobaccos, which suggests lower volatility compounds and thus a greater potential to nucleate particles.

Control experiments performed in the absence of the water in the waterpipe bowl (SI Figure S13a) showed particle number concentration and size distribution that were similar to those when water was present, suggesting that the water does not act as a filter for those particles. This phenomenon was briefly mentioned in a previous study (Monn et al. 2007). This observation is also consistent with previous studies (Hogan et al. 2005; Spanne, Grzybowski, and Bohgard 1999; Wei, Rosario, and Montoya 2010) that demonstrated that the collection efficiency for particles with diameter ranging from 10 to ∼700 nm using the commonly used impinger technique (where the air sample is bubbled through a reservoir containing water, similar to the waterpipe principle) is very small (less than 20% at 1–12 L min^{-1}).

For comparison, Figure 3b presents a typical size distribution of mainstream smoke from the 3R4F reference cigarette and shows that the mode of the distribution is centered around 150 nm for the entire duration of the session. Some ultrafine particles are also present in the cigarette mainstream smoke, but the majority of the particles have diameters larger than 100 nm. It is important to note that the particles from the hookah mainstream smoke likely underwent a higher degree of evaporation during their transport through the dilution system, as it has been reported for e-cigarettes particles compared to reference cigarette (Ingebrethsen, Cole, and Alderman 2012). However, comparison between conditions can still be made.

Ultrafine particles are expected to be deposited in the deepest part of the respiratory tract (Chow and Watson 2007; Hinds 1999). The smallest nanoparticles (<50 nm) can even cross the blood-brain barrier (Betzer et al. 2017; Oberdorster et al. 2004). To compare the potential health impact of ultrafine particles measured for hookah and cigarette mainstream smoke inhaled into the respiratory tract, the particle concentration for different size ranges was determined. Figures 4a–d show the time profile of particles

concentrations with diameter $d < 100$ nm, $d < 70$ nm, $d < 50$ nm, and $d < 20$ nm for the conventional tobacco, charcoal only, the conventional tobacco run without water in the bowl and the reference 3R4F cigarette.

It can be seen that the charcoal itself generated a substantial number of particles of all diameters at a relatively constant concentration during the smoking session. The mainstream smoke from the conventional tobacco experiment showed an enhancement of nanoparticles of all size ranges at the beginning of the smoking session (first 10 min). The increase in the observed particle number concentration is likely due to nucleation from the vapors emitted from the tobacco. As the smoking session proceeds, the particles grow and no new particles are formed, as seen by the decrease in the $d < 20$ nm and $d < 50$ nm particles concentration. This is likely due to the increase in condensation sink caused by the higher concentrations of large particles, which effectively scavenge smaller particles. At the end of the experiments, concentrations of $d < 70$ nm and d < 100 nm particles for the conventional tobacco and charcoal-only are similar.

The experiment performed without water in the bowl showed relatively low particle concentrations at $d < 20$ nm in the first 10 min of the smoking session, but also much lower ultrafine particle concentrations in general. It appears that, rather than acting as a protective filter for the user, the water vapor actually appeared to support new particle formation in the hookah mainstream smoke, likely due to the cooling effect of the water, leading to higher concentrations of ultrafine particles in general and the smallest size classes in particular.

By comparison, cigarette smoke produced fewer particles with $d < 70$ nm compared to the hookah mainstream smoke, as shown in Figure 4c (first 10 min). However, a similar concentration of particles with $d < 100$ nm was observed for both the hookah smoke and the 3R4F reference cigarette.

An averaged dose of ultrafine particles received by one smoker (defined in this study as the total number of particles inhaled in one puff of mainstream smoke) was estimated from the size distribution data for both the hookah and cigarette samples as follows:

$$\text{dose} = C \times \text{dil.factor} \times \text{vol}_{\text{puff}}$$

where C is the total particle concentration (particles per cm^3) measured by the SMPS averaged across all three tobaccos at a time t, *dil. factor* is the averaged dilution factor provided by the sampling system, and vol_{puff} is the volume of one puff of hookah smoke
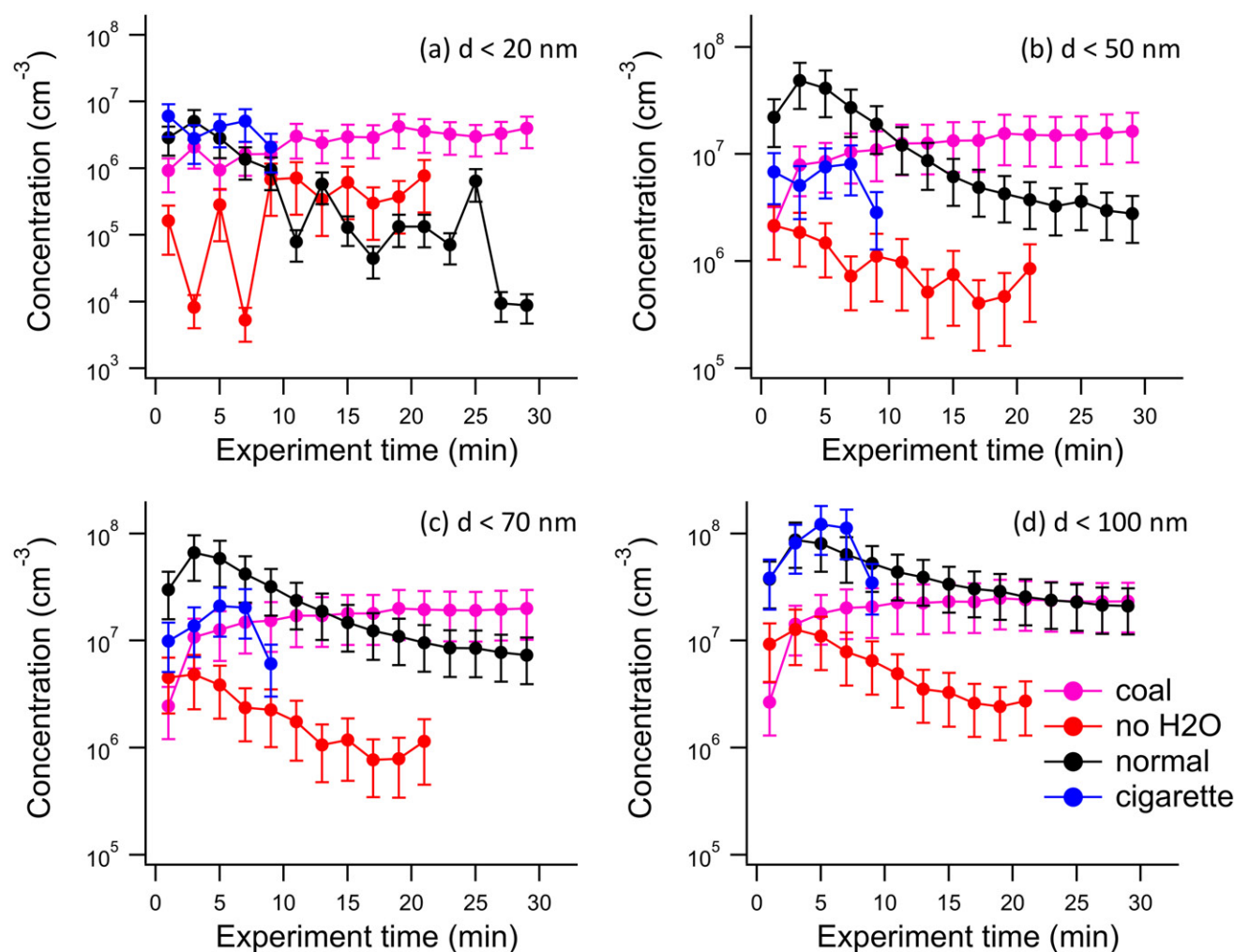
Figure 4. Concentration profile of nanoparticles with diameters $d < 20$ nm (a), $d < 50$ nm (b), $d < 70$ nm (c) and $d < 100$ nm (d) measured in the mainstream smoke as a function of smoking time for the conventional tobacco (black trace; $n = 4$), the coal only experiment (pink trace; $n = 3$), the conventional tobacco with no water (red trace; $n = 2$) and the 3R4F reference cigarette (blue cigarette; $n = 3$). Concentrations are corrected for dilution and for size-dependent transmission losses through the experimental system. Error bars are one standard deviation of the mean.

(860 mL) or cigarette smoke (36 mL). Table 2 shows the comparison between hookah and cigarette total ultrafine particle number received by a smoker for one puff of smoke for each size range. Results showed that the dose of particles received by one smoker was much higher for the hookah mainstream smoke at the beginning of a session than the cigarette mainstream smoke, and the difference increased as the diameter of the particles decreased. Taking the average values for total ultrafine particles inhaled in one puff ($d < 100$ nm), the dose received by one smoker per hookah puff corresponded to smoking 2.4 cigarettes (assuming 7 puffs/cigarette). However, at the very beginning of the hookah session, when the concentration of the particles was the highest, the total particles with $d < 100$ nm and $d < 20$ nm inhaled by one smoker in one puff would be the equivalent of

smoking 5 and 25 cigarettes (assuming 7 puffs/cigarette) respectively. After 10 min, the dose of hookah mainstream smoke particles received by one smoker in one puff was somewhat comparable to the dose from one 3R4F reference cigarette.

3.3. Chemical composition of ultrafine particles in mainstream smoke

The chemical composition of ultrafine particles was measured by TDCIMS. The size-resolved particulate mass distribution collected by the instrument at early times of a hookah smoking session is shown in SI Figure S14, and indicates that the total mass collected on the wire was dominated by particles with diameters ranging from 40–80 nm. The mass spectra obtained for each tobacco evaluated are presented in

Table 2. Averaged dose of particles inhaled by a smoker determined from size distribution measurements as a function of particle diameters defined as the total number concentration of particles contained in 1 puff (hookah puff volume = 860 mL; cigarette puff volume = 36 mL).

Time after starting the session	<100 nm	<70 nm	<50 nm	<20 nm
Normal (n = 8)[a]				
4 min	$9.92\ (\pm 3.5) \times 10^{10}$	$6.07\ (\pm 2.2) \times 10^{10}$	$3.73\ (\pm 1.3) \times 10^{10}$	$2.09\ (\pm 0.8) \times 10^{9}$
15 min	$3.55\ (\pm 1.3) \times 10^{10}$	$1.34\ (\pm 0.5) \times 10^{10}$	$4.83\ (\pm 1.7) \times 10^{9}$	$2.63\ (\pm 0.9) \times 10^{7}$
Average	$4.44\ (\pm 0.8) \times 10^{10}$	$2.13\ (\pm 0.5) \times 10^{10}$	$1.08\ (\pm 0.4) \times 10^{10}$	$3.38\ (\pm 1.5) \times 10^{8}$
No water (n = 2)[b]				
4 min	$1.05\ (\pm 0.6) \times 10^{10}$	$3.71\ (\pm 2.0) \times 10^{9}$	$1.29\ (\pm 0.7) \times 10^{9}$	$2.98\ (\pm 1.5) \times 10^{6}$
15 min	$2.28\ (\pm 1.2) \times 10^{9}$	$4.87\ (\pm 2.5) \times 10^{8}$	$1.36\ (\pm 0.8) \times 10^{8}$	$4.21\ (\pm 3.0) \times 10^{7}$
Average	$4.76\ (\pm 1.0) \times 10^{9}$	$1.45\ (\pm 0.4) \times 10^{9}$	$4.75\ (\pm 1.4) \times 10^{8}$	$2.76\ (\pm 0.6) \times 10^{7}$
No tobacco (n = 3)[c]				
4 min	$9.39\ (\pm 4.6) \times 10^{9}$	$6.46\ (\pm 3.2) \times 10^{9}$	$4.14\ (\pm 2.0) \times 10^{9}$	$3.33\ (\pm 1.7) \times 10^{8}$
15 min	$1.54\ (\pm 0.8) \times 10^{10}$	$1.09\ (\pm 0.5) \times 10^{10}$	$7.22\ (\pm 3.5) \times 10^{9}$	$5.32\ (\pm 2.7) \times 10^{8}$
Average	$1.37\ (\pm 0.2) \times 10^{10}$	$9.92\ (\pm 1.4) \times 10^{9}$	$6.75\ (\pm 1.0) \times 10^{9}$	$5.37\ (\pm 0.9) \times 10^{8}$
Reference cigarette (n = 3)				
Average	$2.68\ (\pm 0.7) \times 10^{9}$	$3.56\ (\pm 1.0) \times 10^{8}$	$7.31\ (\pm 1.8) \times 10^{7}$	$1.17\ (\pm 0.2) \times 10^{7}$

[a]Include all the tobacco (n = 4 for the conventional tobacco; n = 2 for the nicotine-free herbal tobacco; n = 2 for the dark leaf unwashed tobacco).
[b]Conventional tobacco (n = 2).
[c]Includes the run with glycerol in the place of the tobacco.

SI Figures S15(a–c), and the one corresponding the reference cigarette in SI Figure S15d. The upper limit for the m/z range in SI Figure S15 was restricted by the resolution of the mass spectrometer, as it is difficult to unambiguously assign molecular formulas to peaks above m/z 260. The lower limit of m/z 120 was chosen to show primarily unfragmented species rather than ionic fragments. Most ions smaller than this size can have a major thermal decomposition component (as evidenced by their late evolution in the TDCIMS temperature ramp). Figure 5a represents the resulting Kendrick mass defect plot based on CH_2 units derived from the mass spectra obtained for the conventional tobacco mixture compared with the 3R4F reference cigarette sample.

Major observed positive ions can be attributed to sugar or polysacharide derivatives. One of the major peaks observed in the mainstream smoke from the conventional tobacco was at m/z 163.060 corresponding to a chemical composition of $[C_6H_{11}O_5]^+$ (Figures 5a and SI Figure S15a), most likely indicating particulate levoglucosan, a major combustion product of cellulose and also likely arising from the sweetener added to the tobacco. This peak is part of a series of dehydrated compounds that arise from simple monosaccharide, $C_6H_{12}O_6$ (detected as $C_6H_{13}O_6^+$, Figure 5a). The tobacco additive glycerol was likely the dominant semivolatile component of the hookah smoke, evidenced by very large signals in the gas phase background, indicating adsorption from the gas phase onto the filament. Glycerol was sometimes detected as a particle phase component, but the strong gas phase background signal made detection equivocal in many cases and for this reason it was excluded from plots. However, glycerol appeared to form a condensation product ($C_9H_{18}O_8$) with a C_6 monosaccharide in the particle phase, and this product was a major component of the hookah smoke aerosol.

Nicotine ($C_{10}H_{14}N_2$) was also identified in the hookah mainstream particles for both the conventional tobacco and the dark leaf unwashed tobacco, with a protonated molecular ion peak at m/z 163.123 ($[C_{10}H_{15}N_2]^+$). The resolving power of the instrument was sufficient to distinguish it from the adjacent levoglucosan $[C_6H_{11}O_5]^+$ peak t m/z 163.060 (SI Figure S16). A higher fraction of nicotine was measured in the dark leaf unwashed tobacco (SI Figure S15c), which is often observed in unwashed dark leaf tobacco products (Salloum et al. 2015). However, the particle phase nicotine fraction of the cigarette smoke was much higher than for any of the tobacco-generated aerosol (SI Figure S15d). Nicotine was the major identified peak in the cigarette aerosol mass spectrum. Presence of a relatively high amount of nicotine in the particle phase by comparison to gas phase (PTR-ToF-MS measurement described above) is consistent with established gas-particle partitioning of nicotine that favored particle phase in cigarette smoke, and its partitioning can be highly influenced by the temperature and RH of the mainstream smoke (John et al. 2018; Pankow 2001; Pankow et al. 2003).

Overall, the hookah smoke aerosol positive ion TDCIMS mass spectra were very simple, largely containing cyclic saccharide-derived polyols, with very little influence of nitrogen-containing species (Figure 5). This suggests that the actual tobacco was not very efficiently aerosolized and that the additives may actually dominate the composition of generated particles. There were, in general, significant gas phase background signals from many compounds, consistent
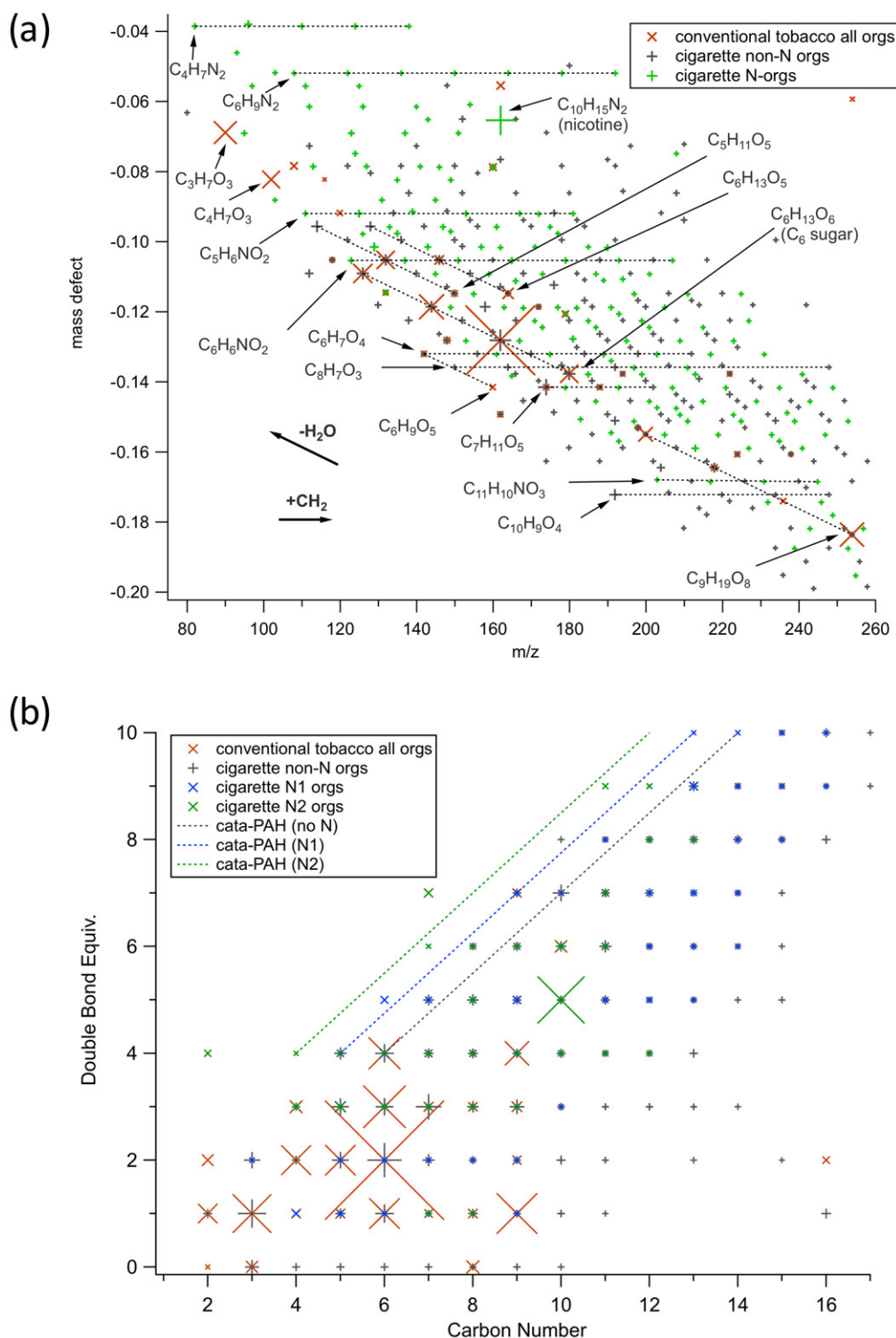
Figure 5. (a) Kendrick mass defect plot based on CH_2 units from TDCIMS measurements and (b) Double bond equivalent plot for TDCIMS-detected ions for respectively two characteristic experiments one with the conventional tobacco using the waterpipe, and one experiment using the 3R4F reference cigarette. In (a), formulas are given in their detected ionic form (as an H^+ adduct) with the charge symbol dropped to avoid clutter. The orange X markers are data from the tobacco, which had almost no major contributions from N-containing molecules. The + markers are from the cigarette experiment, where gray points are non-N organics and green points are N-containing organics. The symbol sizes are scaled to the relative intensity of the peaks in the mass spectra, and only peaks contributing at least 0.1% to the total signal were included. Vectors indicating shifts of CH_2 addition and loss of H_2O are indicated with labeled bold arrows. In (b), the lines correspond to the region where cata-condensed (i.e., least compact) PAHs with 0, 1 or 2 heterocyclic nitrogen respectively would appear. Thus, if a molecule falls in the line or is above the line, then it is most likely a condensed-aromatic.

with the view that a large component of the aerosol was semi-volatile and was likely subjected to evaporation and condensation. The observed homogeneous nucleation of new particles in the hookah mainstream smoke is also consistent with vapor condensation playing a major role. In contrast, the cigarette smoke ultrafine aerosol was much more chemically complicated, with a wide range of oxidation states and degrees of aromaticity (Figure 5b). The detected species in the cigarette smoke had lower gas phase backgrounds, suggesting that they were primarily low-volatility species confined to the particles or that the aerosol was more viscous and retained semivolatile species more effectively than the hookah smoke. The cigarette smoke ultrafine aerosol composition was broadly consistent with that for other types of biomass burning aerosol, for example showing homologous series of heterocyclic reduced-nitrogen species, oxygenated aromatics, alkanoic acids, and polycyclic aromatic hydrocarbons (Laskin, Smith, and Laskin 2009). The major differences between the hookah smoke and cigarette smoke nanoparticles are likely due to the difference in the combustion and volatilization process, involving much lower temperature for the waterpipe than the cigarette (Shihadeh 2003).

4. Conclusions

The results presented in this study advance our understanding of the properties and potential impacts of hookah mainstream smoke. Major components of the measured hookah smoke included glycerol and its decomposition products, dehydrated sugars, and carbon monoxide. We observed large concentrations of ultrafine particles ($d < 100$ nm in diameter), especially during the first 10 min of the smoking session. It is remarkable that the number of ultrafine particles inhaled in a single puff of hookah mainstream smoke is often equivalent to smoking more than one entire cigarette. While the dose-response relationship for the hookah smoke and cigarette smoke are likely to be different (reflecting the different volume of mainstream smoke inhaled by the smoker; 860 mL for the hookah vs 36 mL for the cigarette), the large ultrafine particle number concentration in the former is cause for concern and highlights the potential danger of regular waterpipe smoking.

The chemical composition of the hookah aerosol is also remarkably different from that of a cigarette. The former is dominated by the glycerol and its thermal decomposition products in the gas phase, and by sugar-related molecules in the particle phase. The latter is far more complex reflecting the higher combustion temperature in the cigarette, which generates a huge diversity of toxic compounds, while the low temperature waterpipe process and the practice of adding sugared flavoring and glycerol results in particles that are less concentrated in many toxic compounds. Nevertheless, aside from the significant exposure to carbon monoxide, hookah mainstream smoke is not without health hazard, considering the presence of large amount of glycerol decomposition products in the hookah mainstream smoke, such as acrolein and acetaldehyde, and benzene. Previous studies (Baker and Dixon 2006; Chaouachi 2009; Moldoveannu, Coleman, and Wilkins 2007) showed that the respiratory tract absorbs more than 90% of the mainstream smoke inhaled carbonyl compounds, which have been associated with severe irritations and potential risks for cancer (Feng et al. 2006; IARC 1999). We must also point out that our work only describes relative abundances of the measured chemical compounds and does not quantify doses of specific hookah smoke toxic compounds, which may still be present at levels relevant for human health. Ongoing work using biological models will more directly address health outcomes related to waterpipe smoking.

ORCID

Véronique Perraud (iD) http://orcid.org/0000-0003-1247-9787
Michael J. Lawler (iD) http://orcid.org/0000-0003-0421-6629
Kurtis T. Malecha (iD) http://orcid.org/0000-0002-1438-7440
Rebecca M. Johnson (iD) http://orcid.org/0000-0002-9799-2610
David A. Herman (iD) http://orcid.org/0000-0002-4381-4114
Michael T. Kleinman (iD) http://orcid.org/0000-0003-2724-0066
Sergey A. Nizkorodov (iD) http://orcid.org/0000-0003-0891-0052
James N. Smith (iD) http://orcid.org/0000-0003-4677-8224

References

Akl, E. A., S. Gaddam, S. K. Gunukula, R. Honeine, P. A. Jaoude, and J. Irani. 2010. The effects of waterpipe tobacco smoking on health outcomes: A systematic review. *Int. J. Epidemiol.* 39 (3):834–857. doi:10.1093/ije/dyq002.

Akl, E. A., M. Jawad, W. Y. Lam, C. N. Co, R. Obeid, and J. Irani. 2013. Motives, beliefs and attitudes towards waterpipe tobacco smoking: A systematic review. *Harm Reduct. J.* 10:1–9. doi:10.1186/1477-7517-10-12.

Al Rashidi, M., A. Shihadeh, and N. A. Saliba. 2008. Volatile aldehydes in the mainstream smoke of the narghile waterpipe. *Food Chem. Toxicol.* 46 (11):3546–3549. doi:10.1016/j.fct.2008.09.007.

Aljarrah, K., Z. Q. Ababneh, and W. K. Al-Delaimy. 2009. Perceptions of hookah smoking harmfulness: Predictors and characteristics among current hookah users. *Tob. Induced Dis.* 5 (1):16–22. doi:10.1186/1617-9625-5-16.

Aslam, H. M., S. Saleem, S. German, and W. A. Qureshi. 2014. Harmful effects of shisha: Literature review. *Int. Arch. Med.* 7 (1):16–24. doi:10.1186/1755-7682-7-16.

Baasandorj, M., D. B. Millet, L. Hu, D. Mitroo, and B. J. Williams. 2015. Measuring acetic and formic acid by proton-transfer-reaction mass spectrometry: Sensitivity, humidity dependence, and quantifying interferences. *Atmos. Meas. Tech.* 8 (3):1303–1321. doi:10.5194/amt-8-1303-2015.

Baker, R. R., and M. Dixon. 2006. The retention of tobacco smoke constituents in the human respiratory tract. *Inhal. Toxicol.* 18 (4):255–294. doi:10.1080/08958370500444163.

Betzer, O., M. Shilo, R. Opochinsky, E. Barnoy, M. Motiei, E. Okun, G. Yadid, and R. Popovtzer. 2017. The effect of nanoparticle size on the ability to cross the blood-brain barrier: An in vivo study. *Nanomedicine-UK* 12 (13):1533–1546. doi:10.2217/nnm-2017-0022.

Blair, S. L., S. A. Epstein, S. A. Nizkorodov, and N. Staimer. 2015. A real-time fast-flow tube study of VOC and particulate emissions from electronic, potentially reduced-harm, conventional, and reference cigarettes. *Aerosol Sci. Tech.* 49 (9):816–827. doi:10.1080/02786826.2015.1076156.

Breiev, K., K. M. M. Burseg, G. O'Connell, E. Hartungen, S. S. Biel, X. Cahours, S. Colard, T. D. Mark, and P. Sulzer. 2016. An online method for the analysis of volatile organic compounds in electronic cigarette aerosol based on proton transfer reaction mass spectrometry. *Rapid Commun. Mass Spectrom.* 30 (6):691–697. doi:10.1002/rcm.7487.

Brilli, F., B. Gioli, P. Ciccioli, D. Zona, F. Loreto, I. A. Janssens, and R. Ceulemans. 2014. Proton transfer reaction time-of-Flight mass spectrometric (PTR-TOF-MS) determination of volatile organic compounds (VOCs) emitted from a biomass fire developed under stable nocturnal conditions. *Atmos. Environ.* 97:54–67. doi:10.1016/j.atmosenv.2014.08.007.

Brinkman, M. C., H. Kim, S. S. Buehler, A. M. Adetona, S. M. Gordon, and P. I. Clark. 2018. Evidence of compensation among waterpipe smokers using harm reduction components. *Tob. Control.* 1–9. doi:10.1136/tobaccocontrol-2018-054502.

Brinkman, M. C., H. Kim, J. C. Chuang, R. R. Kroeger, D. Deojay, P. I. Clark, and S. M. Gordon. 2015. Comparison of true and smoothed puff profile replication on smoking behavior and mainstream smoke emissions. *Chem. Res. Toxicol.* 28 (2):182–190. doi:10.1021/tx500318h.

Bruns, E. A., J. G. Slowik, I. El Haddad, D. Kilic, F. Klein, J. Dommen, B. Temime-Roussel, N. Marchand, U. Baltensperger, and A. S. H. Prévôt. 2017. Characterization of gas-phase organics using proton transfer reaction time-of-flight mass spectrometry: Fresh and aged residential wood combustion emissions. *Atmos. Chem. Phys.* 17 (1):705–720. doi:10.5194/acp-17-705-2017.

Cavus, U. Y., Z. H. Rehber, O. Ozeke, and E. Ilkay. 2010. Carbon monoxide poisoning associated with narghile use. *Emerg. Med. J.* 27(5):406–406. doi:10.1136/emj.2009.077214.

Chaouachi, K. 2009. Hookah (shisha, narghile) smoking and environmental tobacco smoke (ETS). A critical review of the relevant literature and the public health consequences. *IJERPH* 6 (2):798–843. doi:10.3390/ijerph6020798.

Chow, J. C., and J. G. Watson. 2007. Overview of ultrafine particles and human health. *WIT Trans. Ecol. Environ.* 99:619–632. doi:10.2495/Rav060601.

Cobb, C., K. D. Ward, W. Maziak, A. L. Shihadeh, and T. Eissenberg. 2010. Waterpipe tobacco smoking: An emerging health crisis in the United States. *Am. J. Health Behav.* 34 (3):275–285. doi:10.5993/Ajhb.34.3.3.

Corma, A., G. Huber, L. Sauvanaud, and P. Oconnor. 2008. Biomass to chemicals: Catalytic conversion of glycerol/water mixtures into acrolein, reaction network. *J. Catal.* 257 (1):163–171. doi:10.1016/j.jcat.2008.04.016.

Dass, C. 1994. Gas-phase fragmentation reactions of protonated glycerol and its oligomers - Metastable and collision-induced dissociation reactions, associated deuterium-isotope effects and the structure of $[C_3H_5O]^+$, $[C_2H_5O]^+$, $[C_2H_4O]^{+\cdot}$ and $[C_2H_3O]^+$ ions. *Org. Mass Spectrom.* 29 (9):475–482. doi:10.1002/oms.1210290906.

de Gouw, J., and C. Warneke. 2007. Measurements of volatile organic compounds in the earths atmosphere using proton-transfer-reaction mass spectrometry. *Mass Spectrom. Rev.* 26(2):223–257. doi:10.1002/mas.20119.

Eichorn, L., D. Michaelis, M. Kemmerer, B. Juttner, and K. Tetzlaff. 2018. Carbon monoxide poisoning from waterpipe smoking: A retrospective cohort study. *Clin. Toxicol.* 56:264–272. doi:10.1080/15563650.2017.1375115.

El-Zaatari, Z. M., H. A. Chami, and G. S. Zaatari. 2015. Health effects associated with waterpipe smoking. *Tob. Control* 24:31–43. doi:10.1136/tobaccocontrol-2014-051908.

Eldridge, A., T. R. Betson, M. V. Gama, and K. McAdam. 2015. Variation in tobacco and mainstream smoke toxicant yields from selected commercial cigarette products. *Regul. Toxicol. Pharm.* 71 (3):409–427. doi:10.1016/j.yrtph.2015.01.006.

Fakhreddine, H. M. B., A. N. Kanj, and N. A. Kanj. 2014. The growing epidemic of water pipe smoking: Health effects and future needs. *Resp. Med.* 108:1241–1253. doi:10.1016/j.rmed.2014.07.014.

Feng, Z. H., W. W. Hu, Y. Hu, and M. S. Tang. 2006. Acrolein is a major cigarette-related lung cancer agent: Preferential binding at p53 mutational hotspots and inhibition of DNA repair. *Proc. Natl. Acad. Sci. USA.* 103 (42):15404–15409. doi:10.1073/pnas.0607031103.

Fitzpatrick, E. M., A. B. Ross, J. Bates, G. Andrews, J. M. Jones, H. Phylaktou, M. Pourkashanian, and A. Williams. 2007. Emission of oxygenated species from the combustion of pine wood and its relation to soot formation. *Process Saf. Environ.* 85 (5):430–440. doi:10.1205/psep07020.

Gordon, S. M., M. C. Brinkman, R. Q. Meng, G. M. Anderson, J. C. Chuang, R. R. Kroeger, I. L. Reyes, and P. I. Clark. 2011. Effect of cigarette menthol content on mainstream smoke emissions. *Chem. Res. Toxicol.* 24 (10):1744–1753. doi:10.1021/tx200285s.

Greaves, J., and J. Roboz. 2014. *Mass spectromtry for the novice.* Boca Raton, FL: CRC Press.

Grekin, E. R., and D. Ayna. 2008. Argileh use among college students in the United States: An emerging trend. *J. Stud. Alcohol Drugs* 69 (3):472–475. doi:10.15288/jsad.2008.69.472.

Grekin, E. R., and D. Ayna. 2012. Waterpipe smoking among college students in the United States: A review of the literature. *J. Am. Coll. Health* 60 (3):244–249. doi:10.1080/07448481.2011.589419.

Hammal, F., A. Chappell, T. C. Wild, W. Kindzierski, A. Shihadeh, A. Vanderhoek, C. K. Huynh, G. Plateel, and B. A. Finegan. 2015. Herbal' but potentially hazardous: An analysis of the constituents and smoke emissions of tobacco-free waterpipe products and the air quality in the cafes where they are served. *Tob. Control* 24 (3):290–297. doi:10.1136/tobaccocontrol-2013-051169.

Haase, K. B., W. C. Keene, A. A. P. Pszenny, H. R. Mayne, R. W. Talbot, and B. C. Sive. 2012. Calibration and inter-comparison of acetic acid measurements using proton-transfer-reaction mass spectrometry (PTR-MS). *Atmos. Meas. Tech.* 5:2739–2750. doi:10.5194/amt-5-2739-2012.

Hemings, E. B., C. Cavallotti, A. Cuoci, T. Faravelli, and E. Ranzi. 2012. A detailed kinetic study of pyrolysis and oxidation of glycerol (propane-1,2,3-triol). *Combust. Sci. Technol.* 184 (7–8):1164–1178. doi:10.1080/00102202.2012.664006.

Hinds, W. C. 1999. *Aerosol technology: Properties, behavior, and measurement of airborne particles.* 2nd ed. New York: John Wiley & Sons.

Hogan, C. J., E. M. Kettleson, M. H. Lee, B. Ramaswami, L. T. Angenent, and P. Biswas. 2005. Sampling methodologies and dosage assessment techniques for submicrometre and ultrafine virus aerosol particles. *J. Appl. Microbiol.* 99 (6):1422–1434. doi:10.1111/j.1365-2672.2005.02720.x.

IARC. 1999. *IARC monographs on the evaluation of carcinogenic risks to Humans - Re-Evaluation of some organic chemicals, hydrazine and hydrogen peroxide.* Lyon, France: IARC Press.

Ingebrethsen, B. J., S. K. Cole, and S. L. Alderman. 2012. Electronic cigarette aerosol particle size distribution measurements. *Inhal. Toxicol.* 24 (14):976–984. doi:10.3109/08958378.2012.744781.

Jamal, A., A. Gentzke, S. S. Hu, K. A. Cullen, B. J. Apelberg, D. M. Homa, and B. A. King. 2017. Tobacco use among Middle and high school students - United States, 2011-2016. *MMWR Morb. Mortal. Wkly Rep.* 66 (23):597–603. doi: dx.doi.org/10.15585/mmwr.mm6623a1. doi:10.15585/mmwr.mm6623a1.

Jawad, M., T. Eissenberg, R. Salman, E. Soule, K. H. Alzoubi, O. F Khabour, N. Karaoghlanian, R. Baalbaki, R. El Hage, N. Saliba, and A. Shihadeh. 2019. Toxicant inhalation among singleton waterpipe tobacco users in natural settings. *Tob. Control* 28 (2):181–188. doi:10.1136/tobaccocontrol-2017-054230.

Jensen, R. P., R. M. Strongin, and D. H. Peyton. 2017. Solvent chemistry in the electronic cigarette reaction vessel. *Sci Rep.* 7:42549–42559. doi:10.1038/srep42549.

John, E., S. Coburn, C. Liu, J. McAughey, D. Mariner, K. G. McAdam, Z. Sebestyen, I. Bakos, and S. Dobe. 2018. Effect of temperature and humidity on the gas-particle partitioning of nicotine in mainstream cigarette smoke: A diffusion denuder study. *J. Aerosol Sci.* 117:100–117. doi:10.1016/j.jaerosci.2017.12.015.

Jordan, A., S. Haidacher, G. Hanel, E. Hartungen, L. Mark, H. Seehauser, R. Schottkowsky, P. Sulzer, and T. D. Mark. 2009. A high resolution and high sensitivity proton-transfer-reaction time-of-flight mass spectrometer (PTR-TOF-MS). *Int. J. Mass Spectrom.* 286 (2–3):122–128. doi:10.1016/j.ijms.2009.07.005.

Karl, T. G., T. J. Christian, R. J. Yokelson, P. Artaxo, W. M. Hao, and A. Guenther. 2007. The tropical Forest and fire emissions experiment: Method evaluation of volatile organic compound emissions measured by PTR-MS, FTIR, and GC from tropical biomass burning. *Atmos. Chem. Phys.* 7 (22):5883–5897. doi:10.5194/acp-7-5883-2007.

Katryniok, B., S. Paul, V. Belliere-Baca, P. Rey, and F. Dumeignil. 2010. Glycerol dehydration to acrolein in the context of new uses of glycerol. *Green Chem.* 12 (12):2079–2098. doi:10.1039/c0gc00307g.

Katurji, M., N. Daher, H. Sheheitli, R. Saleh, and A. Shihadeh. 2010. Direct measurement of toxicants inhaled by water pipe users in the natural environment using a real-time in situ sampling technique. *Inhal. Toxicol.* 22 (13):1101–1109. doi:10.3109/08958378.2010.524265.

Kim, H., M. C. Brinkman, E. Sharma, S. M. Gordon, and P. I. Clark. 2016. Variability in puff topography and exhaled CO in waterpipe tobacco smoking. *Tob. Regul. Sci.* 2 (4):301–308. doi:10.18001/TRS.2.4.2.

Kim, K. H., E. Kabir, and S. A. Jahan. 2016. Waterpipe tobacco smoking and its human health impacts. *J. Hazard. Mater.* 317:229–236. doi:10.1016/j.jhazmat.2016.05.075.[10.1016/j.jhazmat.2016.05.075]

La Fauci, G., G. Weiser, I. P. Steiner, and I. Shavit. 2012. Carbon monoxide poisoning in narghile (waterpipe) tobacco smokers. *Can. J. Emerg. Med.* 14:57–59. doi:10.2310/8000.2011.110431.

Laskin, A., J. S. Smith, and J. Laskin. 2009. Molecular characterization of nitrogen-containing organic compounds in biomass burning aerosols using high-resolution mass spectrometry. *Environ. Sci. Technol.* 43 (10):3764–3771. doi:10.1021/es803456n.

Lawler, M. J., M. P. Rissanen, M. Ehn, R. L. Mauldin, N. Sarnela, M. Sipila, and J. N. Smith. 2018. Evidence for diverse biogeochemical drivers of boreal Forest new particle formation. *Geophys. Res. Lett.* 45 (4):2038–2046. doi:10.1002/2017gl076394.

Lim, B. L., G. H. Lim, and E. Seow. 2009. Case of carbon monoxide poisoning after smoking shisha. *Int. J. Emerg. Med.* 2 (2):121–122. doi:10.1007/s12245-009-0097-8.

Martinasek, M. P., R. J. McDermott, and L. Martini. 2011. Waterpipe (hookah) tobacco smoking among youth. *Curr. Prob. Pediatr. Adolesc. Care.* 41:34–57. doi:10.1016/j.cppeds.2010.10.001.

Martinuzzi, I., Y. Azizi, J. F. Devaux, S. Tretjak, O. Zahraa, and J. P. Leclerc. 2014. Reaction mechanism for glycerol

dehydration in the gas phase over a solid acid catalyst determined with on-line gas chromatography. *Chem. Eng. Sci.* 116:118–127. doi:10.1016/j.ces.2014.04.030.

Maziak, W. 2011. The global epidemic of waterpipe smoking. *Addict. Behav.* 36 (1–2):1–5. doi:10.1016/j.addbeh.2010.08.030.[10.1016/j.addbeh.2010.08.030]

Maziak, W., S. Rastam, I. Ibrahim, K. D. Ward, A. Shihadeh, and T. Eissenberg. 2009. CO exposure, puff topography, and subjective effects in waterpipe tobacco smokers. *Nicotine Tob. Res.* 11 (7):806–811. doi:10.1093/ntr/ntp066.

Mikoviny, T., L. Kaser, and A. Wisthaler. 2010. Development and characterization of a high-temperature proton-transfer-reaction mass spectrometer (HT-PTR-MS). *Atmos. Meas. Tech.* 3 (3):537–544. doi:10.5194/amt-3-537-2010.

Moldoveannu, S., W. I. Coleman, and J. Wilkins. 2007. Determination of carbonyl compounds in exhaled cigarette smoke. *Contrib. Tob. Res.* 22:346–357. doi:10.2478/cttr-2013-0841.

Monn, C., P. Kindler, A. Meile, and O. Brandli. 2007. Ultrafine particle emissions from waterpipes. *Tob. Control* 16 (6):390–393. doi:10.1136/tc.2007.021097.

Monzer, B., E. Sepetdjian, N. Saliba, and A. Shihadeh. 2008. Charcoal emissions as a source of CO and carcinogenic PAH in mainstream narghile waterpipe smoke. *Food Chem. Toxicol.* 46 (9):2991–2995. doi:10.1016/j.fct.2008.05.031.

Muller, M., B. E. Anderson, A. J. Beyersdorf, J. H. Crawford, G. S. Diskin, P. Eichler, A. Fried, F. N. Keutsch, T. Mikoviny, K. L. Thornhill, et al. 2016. In situ measurements and modeling of reactive trace gases in a small biomass burning plume. *Atmos. Chem. Phys.* 16:3813–3824. doi:10.5194/acp-16-3813-2016.

Nimlos, M. R., S. J. Blanksby, X. H. Qian, M. E. Himmel, and D. K. Johnson. 2006. Mechanisms of glycerol dehydration. *J. Phys. Chem. A* 110 (18):6145–6156. doi:10.1021/jp060597q.

Oberdorster, G., Z. Sharp, V. Atudorei, A. Elder, R. Gelein, W. Kreyling, and C. Cox. 2004. Translocation of inhaled ultrafine particles to the brain. *Inhal. Toxicol.* 16:437–445. doi:10.1080/08958370490439597.

Oladhosseini, S., and G. Karimi. 2016. Mathematical modeling of transport phenomena during waterpipe smoking-a parametric study. *Int. J. Multiphase Flow* 85:314–325. doi:10.1016/j.ijmultiphaseflow.2016.06.022.

Pagonis, D., J. E. Krechmer, J. de Gouw, J. L. Jimenez, and P. J. Ziemann. 2017. Effect of gas-wall partitioning in teflon tubing and instrumentation on time-resolved measurements of gas-phase organic compounds. *Atmos. Meas. Tech.* 10 (12):4687–4696. doi:10.5194/amt-10-4687-2017.

Pankow, J. F. 2001. A consideration of the role of gas/particle partitioning in the deposition of nicotine and other tobacco smoke compounds in the respiratory tract. *Chem. Res. Toxicol.* 14 (11):1465–1481. doi:10.1021/tx0100901.

Pankow, J. F., A. D. Tavakoli, W. T. Luo, and L. M. Isabelle. 2003. Percent free base nicotine in the tobacco smoke particulate matter of selected commercial and reference cigarettes. *Chem. Res. Toxicol.* 16 (8):1014–1018. doi:10.1021/tx0340596.

Primack, B. A., J. Sidani, A. A. Agarwal, W. G. Shadel, E. C. Donny, and T. E. Eissenberg. 2008. Prevalence of and associations with waterpipe tobacco smoking among US university students. *Ann. Behav. Med.* 36 (1):81–86. doi:10.1007/s12160-008-9047-6.

Rainey, C. L., J. R. Shifflett, J. V. Goodpaster, and D. Z. Bezabeh. 2013. Quantitative analysis of humectants in tobacco products using gas chromatography (GC) with simultaneous mass spectrometry (MSD) and flame ionization detection (FID). *Contrib. Tob. Res.* 25:576–585. doi:10.2478/cttr-2013-0934.

Retzky, S. 2017. Carbon monoxide poisoning from hookah smoking: An emerging public health problem. *J. Med. Toxicol.* 13 (2):193–194. doi:10.1007/s13181-017-0617-5.

Rezk-Hanna, M., and N. L. Benowitz. 2018. Cardiovascular effects of hookah smoking: Potential implications forcardiovascular risk. *Nicotine Tob. Res.* 00:1–11. doi:10.1093/ntr/nty065.

Roemer, E., H. Schramke, H. Weiler, A. Buettner, S. Kausche, S. Weber, A. Berges, M. Stueber, M. Muench, E. Trelles-Sticken, et al. 2012. Mainstream smoke chemistry and in vitro and in vivo toxicity of the reference cigarettes 3R4F and 3R4F. *Beitr. Tabakforsch. Int.* 25:316–335. doi:10.2478/cttr-2013-0912.

Rogers, T. M., E. R. Grimsrud, S. C. Herndon, J. T. Jayne, C. E. Kolb, E. Allwine, H. Westberg, B. K. Lamb, M. Zavala, L. T. Molina, et al. 2006. On-road measurements of volatile organic compounds in the Mexico City metropolitan area using proton transfer reaction mass spectrometry. *Int. J. Mass Spectrom.* 252:26–37. doi:10.1016/j.ijms.2006.01.027.

Saleh, R., and A. Shihadeh. 2008. Elevated toxicant yields with narghile waterpipes smoked using a plastic hose. *Food Chem. Toxicol.* 46 (5):1461–1466. doi:10.1016/j.fct.2007.12.007.

Salloum, R. G., W. Maziak, D. Hammond, R. Nakkash, F. Islam, X. Cheng, and J. F. Thrasher. 2015. Eliciting preferences for waterpipe tobacco smoking using a discrete choice experiment: Implications for product regulation. *BMJ Open* 5:1–7. doi: ARTN e009497 [CrossRef]10.1136/bmjopen-2015-009497.

Sampson, M. M., D. M. Chambers, D. Y. Pazo, F. Moliere, B. C. Blount, and C. H. Watson. 2014. Simultaneous analysis of 22 volatile organic compounds in cigarette smoke using gas sampling bags for high-throughput solid-phase microextraction. *Anal. Chem.* 86 (14):7088–7095. doi:10.1021/ac5015518.

Sander, R. 2015. Compilation of Henry's law constants (version 4.0) for water as solvent. *Atmos. Chem. Phys.* 15:4399–4981. doi:10.5194/acp-15-4399-2015.

Schroder, D. 2008. Gaseous rust: Thermochemistry of neutral and ionic iron oxides and hydroxides in the gas phase. *J. Phys. Chem. A.* 112:13215–13224. doi:10.1021/jp8030804

Schubert, J., A. Luch, and T. G. Schulz. 2013. Waterpipe smoking: Analysis of the aroma profile of flavored waterpipe tobaccos. *Talanta.* 115:665–674. doi:10.1016/j.talanta.2013.06.022.

Schubert, J., J. Bewersdorff, A. Luch, and T. G. Schulz. 2012a. Waterpipe smoke: A considerable source of human exposure against furanic compounds. *Anal. Chim. Acta.* 709:105–112. doi:10.1016/j.aca.2011.10.012.

Schubert, J., J. Hahn, G. Dettbarn, A. Seidel, A. Luch, and T. G. Schulz. 2011a. Mainstream smoke of the waterpipe: Does this environmental matrix reveal as significant source of toxic compounds? *Toxicol. Lett.* 205 (3):279–284. doi:10.1016/j.toxlet.2011.06.017.

Schubert, J., V. Heinke, J. Bewersdorff, A. Luch, and T. G. Schulz. 2012b. Waterpipe smoking: The role of humectants in the release of toxic carbonyls. *Arch. Toxicol.* 86 (8):1309–1316. doi:10.1007/s00204-012-0884-5.

Schubert, J., O. Kappenstein, A. Luch, and T. G. Schulz. 2011b. Analysis of primary aromatic amines in the mainstream waterpipe smoke using liquid chromatography-electrospray ionization tandem mass spectrometry. *J. Chromatogr. A.* 1218 (33):5628–5637. doi:10.1016/j.chroma.2011.06.072.

Schubert, J., F. D. Muller, R. Schmidt, A. Luch, and T. G. Schulz. 2015. Waterpipe smoke: Source of toxic and carcinogenic VOCs, phenols and heavy metals? *Arch. Toxicol.* 89 (11):2129–2139. doi:10.1007/s00204-014-1372-x.

Sepetdjian, E., R. A. Halim, R. Salman, E. Jaroudi, A. Shihadeh, and N. A. Saliba. 2013. Phenolic compounds in particles of mainstream waterpipe smoke. *Nicotine Tob. Res.* 15 (6):1107–1112. doi:10.1093/ntr/nts255.

Sepetdjian, E., A. Shihadeh, and N. A. Saliba. 2008. Measurement of 16 polycyclic aromatic hydrocarbons in narghile waterpipe tobacco smoke. *Food Chem. Toxicol.* 46 (5):1582–1590. doi:10.1016/j.fct.2007.12.028.

Shihadeh, A. 2003. Investigation of mainstream smoke aerosol of the argileh water pipe. *Food Chem. Toxicol.* 41 (1):143–152. doi: Pii S0278-6915(02)00220-X

Shihadeh, A., S. Azar, C. Antonios, and A. Haddad. 2004. Towards a topographical model of narghile water-pipe cafe smoking: A pilot study in a high socioeconomic status neighborhood of Beirut, Lebanon. *Pharmacol. Biochem. Behav.* 79 (1):75–82. doi:10.1016/j.pbb.2004.06.005.

Shihadeh, A., T. Eissenberg, M. Rammah, R. Salman, E. Jaroudi, and M. El-Sabban. 2014. Comparison of tobacco-containing and tobacco-free waterpipe products: Effects on human alveolar cells. *Nicotine Tob. Res.* 16 (4):496–499. doi:10.1093/ntr/ntt193.

Shihadeh, A., and R. Saleh. 2005. Polycyclic aromatic hydrocarbons, carbon monoxide, "tar", and nicotine in the mainstream smoke aerosol of the narghile water pipe. *Food Chem. Toxicol.* 43 (5):655–661. doi:10.1016/j.fct.2004.12.013.

Shihadeh, A., R. Salman, E. Jaroudi, N. Saliba, E. Sepetdjian, M. D. Blank, C. O. Cobb, and T. Eissenberg. 2012. Does switching to a tobacco-free waterpipe product reduce toxicant intake? A crossover study comparing CO, NO, PAH, volatile aldehydes, "tar" and nicotine yields. *Food Chem. Toxicol.* 50 (5):1494–1498. doi:10.1016/j.fct.2012.02.041.

Shihadeh, A., J. Schubert, J. Klaiany, M. E. Sabban, A. Luch, and N. A. Saliba. 2015. Toxicant content, physical properties and biological activity of waterpipe tobacco smoke and its tobacco-free alternatives. *Tob. Control* 24:22–30. doi:10.1136/tobaccocontrol-2014-051907.

Smith, J. N., K. F. Moore, P. H. McMurry, and F. L. Eisele. 2004. Atmospheric measurements of Sub-20 nm diameter particle chemical composition by thermal desorption chemical ionization mass spectrometry. *Aerosol Sci. Tech.* 38 (2):100–110. doi:10.1080/02786820490249036.

Smith, J. R., S. D. Edland, T. E. Novotny, C. R. Hofstetter, M. M. White, S. P. Lindsay, and W. K. Al-Delaimy. 2011. Increasing hookah use in California. *Am. J. Public Health* 101 (10):1876–1879. doi:10.2105/Ajph.2011.300196.

Sovova, K., K. Dryahina, and P. Spanel. 2011. Selected ion flow tube (SIFT) studies of the reactions of H_3O^+, NO^+ and $O_2^{+\bullet}$ with six volatile phytogenic esters. *Int. J. Mass Spectrom.* 300:31–38. doi:10.1016/j.ijms.2010.11.021.

Spanel, P., and D. Smith. 1997. SIFT studies of the reactions of H_3O^+, NO^+ and O_2^+ with a series of alcohols. *Int. J. Mass Spectrom.* 167:375–388. doi:10.1016/S0168-1176(97)00085-2.

Spanne, M., P. Grzybowski, and M. Bohgard. 1999. Collection efficiency for submicron particles of a commonly used impinger. *Am. Ind. Hyg. Assoc. J.* 60 (4):540–544. doi:10.1202/0002-8894(1999)060 < 0540:CEFSPO>2.0.CO;2.

Stockwell, C. E., P. R. Veres, J. Williams, and R. J. Yokelson. 2015. Characterization of biomass burning emissions from cooking fires, peat, crop residue, and other fuels with high-resolution proton-transfer-reaction time-of-flight mass spectrometry. *Atmos. Chem. Phys.* 15 (2):845–865. doi:10.5194/acp-15-845-2015.

Sutfin, E. L., E. Y. Song, B. A. Reboussin, and M. Wolfson. 2014. What are young adults smoking in their hookahs? A latent class analysis of substances smoked. *Addict. Behav.* 39 (7):1191–1196. doi:10.1016/j.addbeh.2014.03.020.

Veen, M., 2016. Carbon monoxide poisoning caused by waterpipe smoking: A case series. *J. Emerg. Med.* 51 (3):E41–E44. doi:10.1016/j.jemermed.2016.05.046.

Warneke, C., J. M. Roberts, P. Veres, J. Gilman, W. C. Kuster, I. Burling, R. J. Yokelson, and J. de Gouw. 2011. VOC identification and inter-comparison from laboratory biomass burning using PTR-MS and PIT-MS. *Int. J. Mass Spectrom.* 303 (1):6–14. doi:10.1016/j.ijms.2010.12.002.

Wei, Z. C., R. C. Rosario, and L. D. Montoya. 2010. Collection efficiency of a midget impinger for nanoparticles in the range of 3-100 nm. *Atmos. Environ.* 44 (6):872–876. doi:10.1016/j.atmosenv.2009.11.037.

World Health Organization 2015. *Advisory note - Waterpipe tobacco smoking: Health effects, research needs and recommended actions for regulators.* Geneva, Switzerland: WHO document Production services.

Yuan, B., A. R. Koss, C. Warneke, M. Coggon, K. Sekimoto, and J. A. de Gouw. 2017. Proton-transfer-reaction mass spectrometry: Applications in atmospheric sciences. *Chem. Rev.* 117 (21):13187–13229. doi:10.1021/acs.chemrev.7b00325.